



Spatiotemporal variation of intra-urban heat and heatwaves across Greater Sydney, Australia

Sebastian Pfautsch^{a,b,*}, Agnieszka Wujeska-Klause^a, Judi R. Walters^a

^a Urban Studies, School of Social Sciences, Western Sydney University, Australia

^b Urban Transformations Research Centre, Western Sydney University, Australia

ARTICLE INFO

Keywords:

Heatwaves
Microclimate
Weather stations
Western Sydney

ABSTRACT

Rising summer heat and more frequent and intense heatwaves impact countless metropolitan regions, including Greater Sydney, Australia. An analysis of historic air temperature measurements (1859–2020) reveals a notable increase in the number of ‘hot’ (≥ 35 °C) days during austral summers. While in the first 120 years of records 351 hot days were identified, 478 hot days were recorded during 2000–2020 alone. Trajectories of summer heat until 2060 indicate that maximum air temperatures in Western Sydney could be ≥ 35 °C during 160 days.

A second, more granular analysis compared air temperature measurements recorded at 274 urban microsites during the summers of 2019 and 2020 with measurements of official weather stations in Central and Western Sydney. Results revealed that the number of hot (≥ 35 °C), extreme (≥ 40 °C), and ‘catastrophic’ (≥ 45 °C) heat days was markedly greater than those reported by official weather stations. Underreporting of heat was greatest across the Local Government Area (LGA) of Cumberland, where data loggers recorded 32 hot and 15 extreme heat days, compared to 7 hot and 1 extreme heat day recorded by the nearest official station. Based on empirical measurements, a set of novel ‘heat risk’ maps identify suburbs and regions inside LGAs where underreporting of summer heat is high. Findings indicate that communities across Greater Sydney are exposed to more frequent and more intense heat than previously reported. Underreporting of local urban heat results in lower preparedness and thus higher risk of harm to urban populations of Greater Sydney and likely many other metropolitan regions.

1. Introduction

As the planet warms, the frequency, intensity and duration of extreme heat events has increased in many areas around the world (Jyoteeshkumar Reddy et al., 2021) and is expected to increase further in the coming decades (IPCC et al., 2023). Extreme heat events in cities causes a rise in public health risks (Marinaccio et al., 2019) and leads to increased rates of mortality and morbidity (Madrigano et al., 2015; Khatana et al., 2022). In 2022, India, Pakistan, the USA, China, and Europe all recorded extreme heat events, with an estimated 61,672 heat-related deaths in Europe alone (Ballester et al., 2023). Widespread and long-lasting extreme heat events were also recorded during the summer of 2023 across large parts of the northern hemisphere. These two consecutive hot summers impacted billions of people, making it clear that extreme heat is now a reality even in countries that traditionally have cooler climates such as the United Kingdom and Canada. Heat-related mortality will rise in the future unless steps are taken to protect people from thermal extremes (Vicedo-Cabrera et al., 2021),

especially those that have high heat vulnerability including the elderly, sick, frail, and very young (Zanobetti et al., 2013; Lu et al., 2021). As the global human population is living increasingly urban lifestyles, a refined understanding of intra-urban patterns of heat is needed to assist local populations better adapt to extreme heat conditions.

Measurement of urban heat that is most relevant to human-health outcomes usually focusses on canopy-layer air temperatures (Li et al., 2024) and compares differences between urban and non-urban areas to quantify heat island effects. Intensities of canopy-layer urban heat island (CLUHI) effects of 6–7 °C have been recently reported for Bangkok, Thailand (Marks and Connell, 2023), and 7–9 °C in the Angul-Talcher region in India (Singh et al., 2023). Observations of CLUHI effects have traditionally used meteorological weather station networks embedded in cities. There are two main problems with using these networks for urban heat studies: first, they are limited to a very small number of stations inside a city (e.g., six stations used in Lecce, Italy by Donato et al., 2023); and second, they must, according to the World Meteorological Association (2018), be located in an open area away

* Corresponding author. Urban Studies, School of Social Sciences, Western Sydney University, Australia.

E-mail address: S.Pfautsch@westernsydney.edu.au (S. Pfautsch).

<https://doi.org/10.1016/j.wace.2024.100741>

Received 26 April 2024; Received in revised form 15 November 2024; Accepted 8 December 2024

Available online 9 December 2024

2212-0947/© 2024 The Authors. Published by Elsevier B.V. This is an open access article under the CC BY license (<http://creativecommons.org/licenses/by/4.0/>).

from the built environment. Thus, meteorological measurements may not represent the complexity of finer-scale temperature variability across the various microclimates in the canopy layer (Stewart and Oke, 2012), leading to an inability of measurements to monitor heat where people live and work (Li et al., 2024). More recently, these problems have been overcome through application of meteorological measurement networks with a higher density where sensors are embedded into the urban landscape. For example, the CLUHI effect was quantified using a network of 17 sensors located on building rooftops in Rome, Italy (Cecilia et al., 2023), and by 60 sensors in Dijon, France (Richard et al., 2021). Higher levels of data granularity have also been achieved in some major cities through networks such as the HiSAN in Tainan, Taiwan (Chen et al., 2024), and the Extended METROS in Tokyo, Japan (Honjo et al., 2015), where networks of up to 200 sensors collect highly spatiotemporal CLUHI effect data.

Increasing the spatial resolution of empirical measurements of near-surface urban air temperatures even more is possible when accessing crowd-sourced data from citizen weather stations (CWS). This relatively novel approach uses data packages from third-party providers. For example, in Zurich, Switzerland, data from 634 CWS were used to model urban air temperatures during an extreme heat event in June 2019 (Zumwald et al., 2021). A research team in Sydney, Australia, used empirical measurements from 492 CWS to elucidate the influence of geography and dominant urban typologies on microclimates (Potgieter et al., 2021). Both studies highlight that specific statistical procedures are required to improve reliability of crowd-sourced weather data, yet in-situ observations at fine scales remain scarce (Gubler et al., 2021). Besides methods using empirical data, CLUHI effects and variation of near-surface air temperatures can also be predicted with high spatial resolution using numerical simulations (Yin et al., 2024), computational fluid dynamics (e.g., Back et al., 2023) and models based on Temporal Fusion Transformer neural networks (Zhu et al., 2024).

1.1. Heat in greater sydney

Heatwaves in Australian cities have already increased in frequency, intensity, and duration (Trancoso et al., 2020; Adnan et al., 2022). Like the global trend, it is predicted that in the coming decades, extreme heat events in Australia will occur more often (Steffen et al., 2019; Hughes et al., 2020). Across Greater Sydney - an area of ~12,000 km² and home to 6 million people - maximum, minimum, and mean air temperatures were markedly higher between 2001 and 2016 than in the preceding 30 years (Livada et al., 2019). On January 4, 2020, the LGA of Penrith in Sydney was the hottest place on earth, reaching 48.9 °C (Bureau of Meteorology, 2021), and similarly extreme heat events and trends are predicted to continue and accelerate in the coming years (Melville-Rea and Verschuer, 2022).

Heat in Sydney is strongly influenced by complex synoptic weather patterns, which are influenced by topography, rainfall patterns, and the coastal location (He et al., 2020; Yun et al., 2020). Typically, during summer, afternoon sea breezes keep the eastern parts of Sydney cool, but the built-up environment of the city prevents these breezes from reaching central or western parts of Greater Sydney. This results in high spatiotemporal variability of air temperatures across the city (Yenneti et al., 2020) and makes inland settlements of Greater Sydney naturally hotter than the eastern coastal suburbs. Rapid and widespread transformation of open vegetated space to sprawling settlements in western areas further amplifies baseline warming and the risk of urban overheating and extreme heat events (Khan et al., 2021). Heatwaves in inland settlements of Greater Sydney tend to be longer and more intense than in areas closer to the coast (He et al., 2020; Santamouris et al., 2017; Sadeghi et al., 2018; Steffen et al., 2019). For example, Kong et al. (2023) showed that mean air temperatures in Parramatta (Central Sydney) were up to 3.2 °C hotter than those in the Sydney Central Business District during a heatwave in 2020. Therefore, health outcomes of the aging population in the inland region are expected to be severely

impacted by increasing heat (Gee and Gissing, 2021).

1.2. Heat preparedness

Increases in morbidity and mortality due to extreme heat are largely preventable if effective public health interventions (Bassil and Colet, 2010) and cooling strategies (Chaston et al., 2022) are implemented. Preparedness is key for enabling emergency services to respond to future extreme heat events and keep people safe. Demand for space cooling dramatically increases during extreme heat events and is most pronounced in urban areas. In Sydney, the 2020 heatwave caused an increase in cooling degree hours of 60% (Li et al., 2023), which placed significant strain on electricity grid. This in turn increases the risk for blackouts with serious negative impacts on public health (Stone Jr. et al., 2023). Equally important is public broadcasting of potential heat risks to support vigilance of carers and local communities. Recognition of this has led to the development of numerous heatwave early warning systems, which are being implemented around the world to improve heat resilience in cities (Kotharkar et al., 2022).

The Australian Bureau of Meteorology (BoM) defines a heatwave as an event “when the maximum and the minimum temperatures are unusually hot over a 3-day period at a location” (*sensu* Bureau of Meteorology, 2022a). The Heatwave Service for Australia (Bureau of Meteorology, 2022b) is responsible for notifying local emergency services and health authorities in the days leading up to predicted heatwave events that are classified as ‘low intensity’, ‘severe’, or ‘extreme’. The Heatwave Service relies on predictive modelling, which in turn requires air temperature data collected from official meteorological weather station networks. Across Greater Sydney, this network consists of 23 stations. It has been reported that the current network of stations lacks the spatial density required to detect thermal variation at a local (intra-urban) scale (Muller et al., 2013; Pfautsch et al., 2023). As previously mentioned, these official weather stations are sited according to standards of the World Meteorological Organisation (WMO), wherein stations are purposely located in open spaces unobstructed by tall trees, human-made surfaces, and buildings (WMO, 2018). Such locations are difficult to find in dense urban areas (Potgieter et al., 2021), meaning that a small number of weather stations are used to represent large, highly heterogeneous areas (Muller et al., 2013; Bahi et al., 2020). Air temperatures recorded by official weather stations can be significantly lower than those collected in densely populated urban areas (Yenneti et al., 2020). Thus, it is likely that urban populations are regularly exposed to more extreme air temperatures than reported. The magnitude of discrepancies between the official measurement network and ambient air temperatures experienced by the population has not been quantified for Greater Sydney. The potential effectiveness of a heat warning system for Greater Sydney is therefore limited, and under-reporting of heat could put vulnerable individuals and even entire local populations at risk during current and future extreme heat events.

1.3. Aim of this study

The aim of this study was to quantify the severity of underreporting of high air temperatures across diverse urban landscapes in Central and Western Sydney using empirical data. Here we define Western Sydney as the area of Greater Sydney that is located to the west, south, and north of the City of Parramatta. This definition is commonly used by urban planners and economists when distinguishing eastern from western Sydney. This research compared air temperature data from official weather stations and their deviation from measurements collected at nearly 300 locations across four LGAs during summer. While climate gradients and the extent of urban overheating across Greater Sydney has been documented (e.g., Yenneti et al., 2020; Khan et al., 2021; Melville-Rea and Verschuer, 2022; Ulpiani et al., 2022; Kong et al., 2023), here we focus on the extent and associated risks of underreporting high and extreme air temperatures. The consequence of this

underreporting would be that predictive heat modelling to issue public warning messages could be insufficient to protect urban populations from heat-related risks.

2. Materials and methods

2.1. Study areas

This work focussed on four LGAs in the Greater Sydney Basin, New South Wales, Australia (Fig. 1). The regional climate across the Basin is humid/sub-tropical (Cfa in the Köppen climate classification). Summers are typically hot and humid: winters are mild and dry. The summer season lasts around 4 months each year (late November to late March), with average daily maximum air temperatures above 25 °C. January is usually the hottest month, with daily maximums above 26 °C and minimums of around 20 °C (Weather Spark, 2022). During summer days, a natural temperature gradient exists from the coastal region in the east where the air is cooler to the inland western region where it is warmer. Based on long-term observations (1900–2012), mean annual precipitation across the Basin is 951 mm, with substantial spatial variation (Herron et al., 2018). The coastal and southern regions of the basin generally receive much higher rainfall per year (>1 300 mm) than the west and northwest (<700 mm).

The selected LGAs represented two central areas where the density of urban infrastructure is increasing (Cumberland and Parramatta), as well as two areas in the far west and southwest of Greater Sydney where large-scale greenfield development is rapidly changing the composition of the urban fringe zone (Penrith and Campbelltown). The associated population growth across the central and western regions of metropolitan Sydney has been remarkably high over the past decade and is expected to continue for many years (Table S1).

2.2. Bureau of Meteorology air temperature data

Daily maximum air temperature (T_{\max}) data for the interval from 1859 to the end of 2020 were obtained for the official weather stations that were inside or closest to the four LGAs in Sydney's central and western regions (Table S2). The LGA of Parramatta was represented by the weather station in Parramatta North, and the LGA of Cumberland was represented by the weather station at Sydney Olympic Park. Like previous studies of the natural thermal gradient spanning east-west across Greater Sydney (e.g., Santamouris et al., 2017; Ulpiani et al., 2021), we also used the weather station at Observatory Hill in eastern Sydney as a comparison (Fig. 1). This weather station captures the weather conditions as Sydney's Central Business District (CBD) and is referred to as Sydney CBD from here on.

The temperature thresholds we used were adopted from BoM climate extreme analyses (<http://www.bom.gov.au/climate/change/about/extremes.shtml>), which are based on temperatures relevant to human physiology. A maximum air temperature of 35 °C is the limit considered safe for humans (Sherwood and Huber, 2010), and heat stress is considered 'extreme' at temperatures above 40 °C (Asseng et al., 2021). From this, any day where T_{\max} was ≥ 35 °C was counted as a 'hot' day, $T_{\max} \geq 40$ °C was an 'extreme heat' day, and $T_{\max} \geq 45$ °C was a 'catastrophic' day.

Using these temperature thresholds, results from daily maximum air temperature data obtained were used to analyse historic trends (from 1859 to 2020) and contemporary changes throughout the two hottest decades within record (2000–2020). From the data recorded by the official weather stations between 2000 and 2020, we calculated the number of hot and extreme heat days in summer (November–March) along the east-west transect in Greater Sydney using linear correlation models (Table 1). We determined the model equations based on the

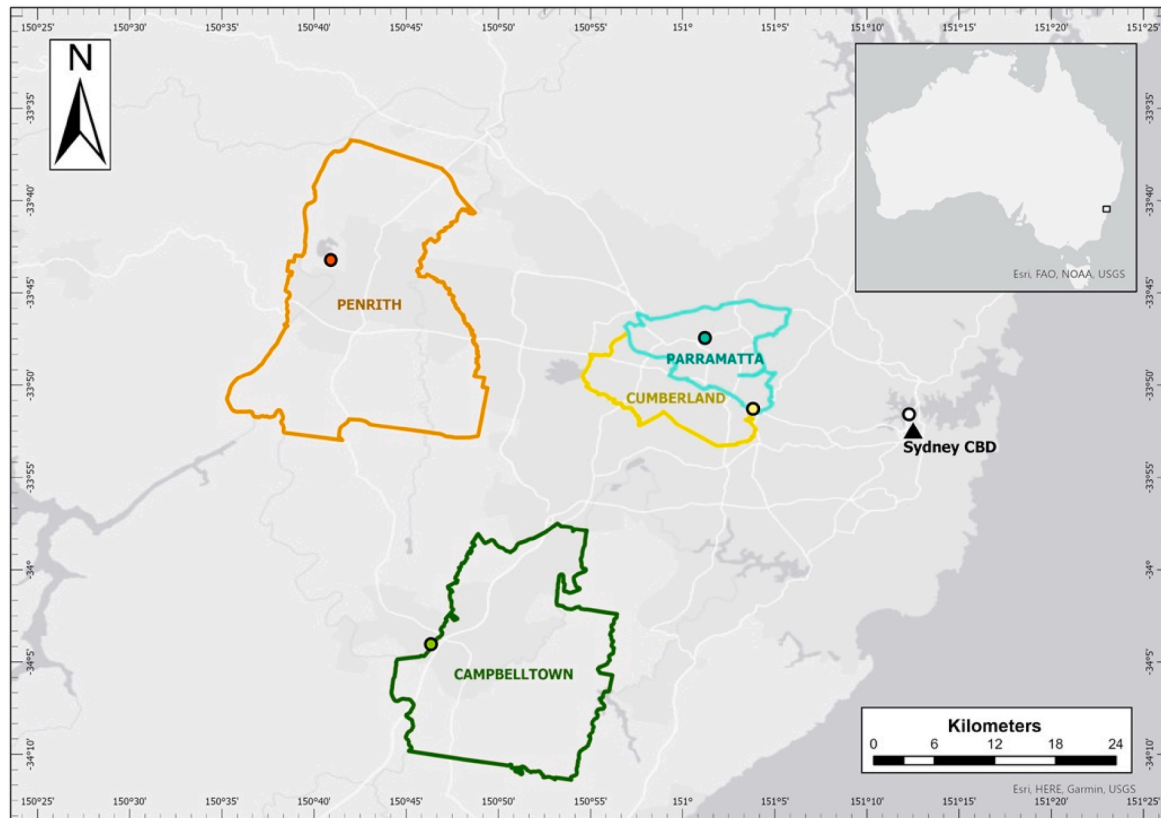


Fig. 1. Location of Local Government Areas (LGAs) and associated Bureau of Meteorology weather stations across the Greater Sydney Basin used in this study. LGAs and weather stations matched by colour: Cumberland = yellow, Parramatta = cyan, Campbelltown = green, Penrith = orange; Sydney Central Business District (CBD, station at Observatory Hill) = white circle.

Table 1

Details for regression models used to estimate the possible number of hot ($T_{max} \geq 35^\circ\text{C}$ and extreme heat days ($T_{max} \geq 40^\circ\text{C}$) for five location in Greater Sydney. The models were based on the number of hot and extreme heat days recorded by Bureau of Meteorology weather stations during summer (November–March). As the decade 2010–2020 was the hottest ever recorded, two time intervals were used, namely 2000–2020 and 2010–2020. Significance of the relationship between year and the number of hot or extreme heat days was set at $p > 0.1$ (*), >0.05 (*), >0.01 (**). Abbreviations: DF = degrees of freedom, RSE = residual standard deviation, CBD = Sydney CBD, represented by the weather station at Observatory Hill, OLY = Olympic Park, PAR = Parramatta, CAM = Campbelltown, PEN = Penrith.

T_{max}	Time interval	Location	DF	RSE	F-statistic	slope	intercept	R^2	p-value
$\geq 35^\circ\text{C}$	2000–2020	CBD	19	2.76	7.39	0.27	1.70	0.28	0.014*
		OLY		4.97	1.76	0.24	8.77	0.09	0.200
		PAR		6.10	2.10	0.32	10.6	0.10	0.164
		CAM		7.47	4.08	0.54	11.49	0.18	0.058*
		PEN		9.38	7.20	0.91	13.84	0.28	0.015*
	2010–2020	CBD	9	2.58	10.60	0.80	0.93	0.54	0.001**
		OLY		5.37	1.41	0.61	8.71	0.14	0.265
		PAR		6.54	2.81	1.04	8.91	0.24	0.128
		CAM		8.01	3.61	1.45	11.09	0.29	0.089*
		PEN		8.96	7.89	2.40	13.15	0.47	0.02*
$\geq 40^\circ\text{C}$	2000–2020	CBD	19	0.68	1.26	0.03	0.22	0.06	0.276
		OLY		1.59	3.54	0.11	0.77	0.16	0.075*
		PAR		2.10	1.29	0.09	1.53	0.06	0.271
		CAM		2.28	3.35	0.15	1.49	0.15	0.083*
		PEN		3.60	7.99	0.37	1.35	0.30	0.011*
	2010–2020	CBD	9	0.78	1.22	0.00	1.22	0.12	0.299
		OLY		2.01	1.09	0.20	1.25	0.11	0.324
		PAR		2.57	0.55	0.18	1.82	0.06	0.476
		CAM		2.49	0.85	0.22	2.60	0.09	0.382
		PEN		3.62	6.40	0.87	1.58	0.42	0.032*

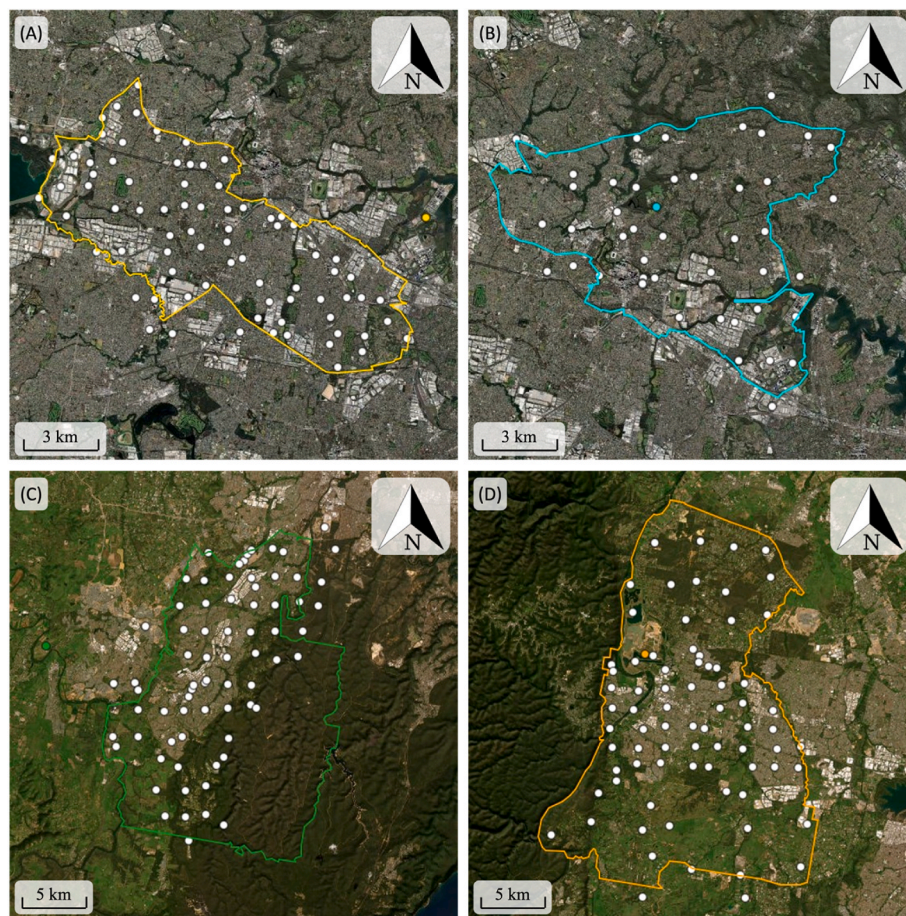


Fig. 2. Location of microclimate temperature loggers (white dots) in four Local Government Areas (LGAs) in Central and Western Sydney. (A) Cumberland, (B) Parramatta, (C) Campbelltown, (D) Penrith. Boundaries of LGAs are shown as solid lines and their colour matches those in Fig. 1. Locations of the nearest official weather stations are also shown as coloured dots.

number of potential hot and extreme heat days recorded between the summer seasons of 1999/2000 (Scenario 1) or 2009/2010 (Scenario 2) and 2019/2020. Models for all five locations (i.e., Sydney CBD, Olympic Park, Parramatta, Campbelltown, and Penrith) had positive intercepts and their slopes increased from eastern to western locations. Relationships were used to estimate the anticipated number of hot and extreme heat days for 2030, 2040, 2050, and 2060.

For this study, the following simplified heatwave definition was adopted: three or more consecutive days where $T_{\max} \geq 35^\circ\text{C}$. We interrogated data from the five BoM weather stations together with custom-made air temperature loggers (see Section 2.4. for details) for the frequency, duration, and intensity of heatwaves recorded between 2000 and 2020.

2.3. Microsite analyses

This study used custom-made air temperature loggers, designed and manufactured at Western Sydney University. Each air temperature logger (ATL) consisted of a water-resistant, single-use temperature sensor (Tempmate S1 V2, Imtec Messtechnik, Heilbronn, Germany) and a reflective weather shield that protected the sensor from direct solar radiation. Technical information and calibration of the device is published elsewhere (Pfautsch et al., 2023). The accuracy of the sensor was 0.5°C and temperatures were recorded every 10 min at 0.1°C resolution.

ATLs were used to record near-surface air temperature at 274 microsites between 1 January and February 28, 2019 across the LGAs of Parramatta ($n = 48$), Cumberland ($n = 79$) and Campbelltown ($n = 72$), and from 1 January to February 29, 2020 across Penrith ($n = 75$).

The ATLs were installed approximately 2.5–3.5 m above ground level on branches of trees or light poles in public spaces. Previous analyses showed that there is no detectable effect on measurements if ATLs are installed in the sun or shade (Pfautsch et al., 2023). All locations were identified by projecting a rectangular grid on the area covered by the LGA. An ATL was placed on the nearest tree or pole at each grid intersection. Grid distances varied with the area covered by the LGA (Fig. 2).

In the LGA of Parramatta, Cumberland and Penrith, a single ATL was installed near official weather stations to be used for quality control of measurements. Correlation analyses of data from ATLs against those recorded by official weather stations yielded coefficients of determination >0.98 (see Pfautsch and Rouillard, 2019a, b; Pfautsch et al., 2020, 2023), indicating very high accuracy of the ATLs. The Mean Absolute Error of these correlations ranged from 0.54 to 1.50 and their Root Mean Squared Error from 0.79 to 1.83 (details are provided in Table S3). To further evaluate the comparability of measurements from ATLs against data recorded by official weather stations, we analysed how frequent ATLs recorded temperatures above or below weather station data, applying the $\pm 0.5^\circ\text{C}$ range of the sensor's accuracy. These analyses utilised measurements collected at official weather stations and ATLs at 3pm. The distinct time point allowed direct comparisons of 226 ATLs against three weather stations (Olympic Park, Campbelltown and Penrith). The weather station at Parramatta did not record 3pm measurements. Location metadata for all microsites is provided in Table S4.

The loggers recorded a total of 2,299,248 air temperature measurements during the study period. Data from ATLs were used to count the number of hot, extreme heat, and catastrophic days as described above for BoM data. The resulting data were used to visualise the discrepancy between the number of hot days reported by ATLs versus those reported by official weather stations for each of the four LGAs. 'Heat risk' maps with spatially interpolated data were created using the *leaflet* R package (version 2.2.2) and the ESRI World Imagery open-source background map. The interpolation procedure used inverse distance weighted (IDW) interpolation method (*gstat* function in *gstat* R package), using a minimum of 10 and a maximum of 12 neighbouring measurement points. The procedure yields continuous raster data for an LGA that is processed

(*interpolate* function in *terra* R package) to generate a map layer at resolution of 20 pixels (*rast* function in *terra* R package).

2.4. Statistical analyses

Regression analyses were used to investigate historic, contemporary, and future trends of the number of hot and extreme heat days across Greater Sydney. Related statistical analyses were conducted using the *lm* function in the *stats* package of R (Version 3.6.0; R Foundation for Statistical Computing, Vienna, Austria). A *t*-test was used to evaluate the relationship between the hot and extreme heat days recorded between 1859 and 2020. Regression analyses were also used to interrogate the relationship among data recorded by BoM stations and ATLs when BoM stations recorded daily $T_{\max} \geq 35^\circ\text{C}$.

3. Results

3.1. Heat recorded by Bureau of Meteorology weather stations

3.1.1. Historic air temperature records

The historic records of maximum daily air temperatures from the five weather stations indicate that the number of hot and extreme heat days has increased in the recent past (Fig. 3A). Given the lack of weather station locations in the central and western region of Greater Sydney until the late 1960s and early 1970s, it is not surprising that the number of hot and extreme days remains relatively low for the first 119 years

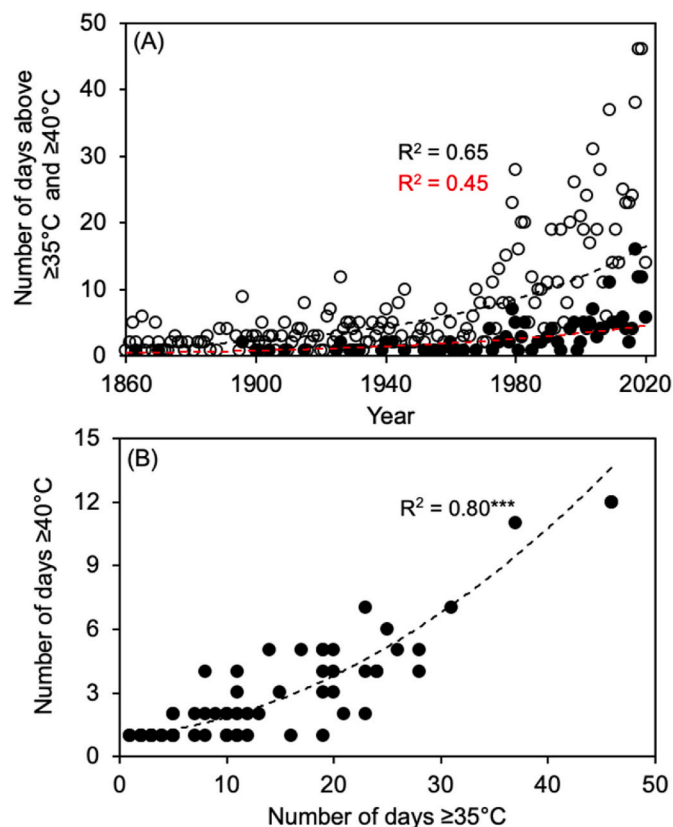


Fig. 3. Hot ($T_{\max} \geq 35^\circ\text{C}$) and extreme heat ($T_{\max} \geq 40^\circ\text{C}$) days across the Greater Sydney Basin. (A) Historic weather data showing the total number of days per year where air temperatures were $\geq 35^\circ\text{C}$ (circles) and $\geq 40^\circ\text{C}$ (dots) for each calendar year between 1859 and 2020. The data were recorded at the five locations listed in Table S2. The dashed lines indicate curvilinear fits, and their respective coefficient of determination is shown; (B) Relationship between the number of hot and extreme heat days. The dashed line indicates the curvilinear fit and the coefficient of determination is shown; asterisks indicate the relationship was highly significant ($p < 0.0001$).

(1859–1978). During this time, maximum air temperatures at Sydney CBD reached $\geq 35^\circ\text{C}$ on 351 days and $\geq 40^\circ\text{C}$ on 32 days before the first major heat events in southwestern Sydney were recorded with 23 hot days and 7 extreme heat days in a single year (1979 at Campbelltown). In the following two decades (1980–1999), the number of hot and extreme heat days was greater than those recorded during the previous 120 years (311 hot days; 48 extreme heat days). The first two decades of the 2000s were even hotter, with 478 hot and 115 extreme heat days. Correlation analyses showed that the relationship between hot and extreme heat days was highly significant ($p > 0.001$) and positive curvilinear, indicating a greater increase in extreme heat days compared to the number of hot days (Fig. 3B).

3.1.2. Heat during 2000–2020

Based on the data from BoM weather stations, the two decades between 2000 and 2020 were the hottest ever recorded in Greater Sydney, and the decade from 2010 to 2020 was hotter than the previous one. The number of hot, extreme heat, and catastrophic days increased at all five weather stations (Table 2). The trend for less extreme heat in eastern Sydney compared to western and southwestern Sydney prevailed. The number of hot, extreme heat, and catastrophic days, and the number of heatwaves increased from Sydney CBD in the east to Penrith in the west during both decades. Also, heatwaves lasted longer and had higher T_{max} during 2010–2020 compared to 2000–2009 (Table 2). At Penrith, the frequency of heatwaves increased from 21 to 26 days, the duration of the longest heatwave increased from 6 to 9 days, and the mean maximum air temperature during heatwaves increased 1.4°C from 40.8°C to 42.2°C . Similar, yet less intense trends, were also found for Campbelltown and Parramatta.

Heat also intensified at the cooler reference location in eastern Sydney. For example, the number of extreme heat and catastrophic days recorded at Sydney CBD doubled between 2000–2009 and 2010–2020 (Table 2). Catastrophic heat was recorded for the first time ever in the Sydney CBD on January 18, 2013 (45.8°C) and at Olympic Park on January 4, 2020 (47.1°C) in the 2010–2020 interval. In comparison, until the end of 2020, not a single heatwave had ever been recorded at this location. Across Greater Sydney, heat records were broken at the end of an extreme heatwave on January 7, 2018, where maximum air temperatures reached catastrophic levels in Penrith (47.3°C), Parramatta (45.0°C), and Campbelltown (45.7°C). These temperature records were exceeded only 2 years later: on January 4, 2020, a temperature of 48.9°C was recorded at the Penrith BoM station. All other stations except Observatory Hill recorded catastrophic T_{max} on the same day (Olympic Park: 47.1°C , Parramatta: 47.0°C , Campbelltown: 46.2°C).

3.1.3. Heat forecast 2030–2060

Based on the period spanning 2000–2020, the number of hot days measured per year at Observatory Hill could increase from 10 in 2030 to 18 in 2060 (Fig. 4A). During the same time interval in Penrith, the

number of hot days could increase from 56 to 100 (Fig. 4A), and the number of extreme heat days rise from 13 to 24 (Fig. 4C). The anticipated number of hot days per year could more than double at most locations and for most decades (Fig. 4B). The ‘worst case scenario’ indicated that in 30–40 years, central and south-western Sydney (Olympic Park, Parramatta, Campbelltown) might experience 13–16 days of extreme heat every year, and western Sydney (Penrith) could see 55 days per annum where T_{max} is $\geq 40^\circ\text{C}$ (Fig. 4D).

3.2. Heat recorded at microsities

During January and February, ATLS across the 226 locations in Cumberland, Campbelltown and Penrith recorded 3pm air temperatures greater 0.5°C than measurements recorded by official weather stations for 30 days and lower than 0.5°C during 14 of the measurement intervals of 59 (2018/19) and 60 days (2019/20). For the remaining 16 days, measurements of ATLS fell within the $\pm 0.5^\circ\text{C}$ temperature threshold of 3pm air temperatures recorded by the official weather stations. The large proportion of days where measurements were recorded outside the threshold for accuracy as per the manufacturer of the ATLS provides confidence that the low-cost loggers did record valid data.

T_{max} across each of the four LGAs varied among microsities. Individual absolute T_{max} recorded by ATLS on the single hottest day in January and February showed that temperatures varied as much as 8°C across an individual LGA. An in-depth analysis of this variability is provided in the Supplementary Materials. Here, the focus is on identifying and quantifying the issue of underreporting of T_{max} by BoM weather stations in urban locations.

Underreporting of the number of hot and extreme heat days by BoM weather stations was widespread, and there was not a single day when all microsities were either recording the same T_{max} or lower T_{max} than the BoM stations. Underreporting was most pronounced across Cumberland where the BoM station recorded $T_{\text{max}} \geq 35^\circ\text{C}$ for 7 days in January and February in 2019, while the ATLS recorded $T_{\text{max}} \geq 35^\circ\text{C}$ for 32 days (Table 3). At this LGA, the number of extreme heat days was 15 times greater than what the BoM weather station had recorded. The weather station at Parramatta did not record a single extreme heat day, whereas the ATLS recorded seven such days. Extreme heat days at Campbelltown were 5 times more frequent at the microsities compared to the closest BoM weather station (Table 3). In Penrith, the number of days when extreme heat and catastrophic T_{max} were recorded were similar at the microsities and the weather station during January and February 2020 (Table 3). At all LGAs, the ATLS captured more frequent and longer lasting heatwaves compared to the BoM weather stations. For the majority of LGAs, the longest heatwave ($T_{\text{max}} \geq 35^\circ\text{C}$) was 5 days but the heatwave at Campbelltown lasted for 10 consecutive days (21–31 January 2019; Table 3).

Subtracting the number of days where individual ATLS recorded $T_{\text{max}} \geq 35^\circ\text{C}$ from those when the reference BoM stations recorded T_{max}

Table 2

Metrics of extreme heat across the Greater Sydney Basin during the past two decades. The number of days where maximum air temperature was $\geq 35^\circ\text{C}$ (hot days), $\geq 40^\circ\text{C}$ (extreme heat days) and $\geq 45^\circ\text{C}$ (catastrophic heat days) recorded by five Bureau of Meteorology weather stations are shown for each decade. The number of heatwaves (#HW) for each decade is provided with the longest duration of a single heatwave (consecutive days where T_{max} was $\geq 35^\circ\text{C}$) in parentheses. Also shown are the mean maximum air temperatures for all heatwaves (mean HW T_{max} (± 1 standard deviation)) and the absolute maximum air temperature (abs T_{max}) recorded in that decade. Stations are listed from east (top, coastal) to west (bottom, inland): CBD = Sydney CBD, represented by the weather station at Observatory Hill, OLY = Olympic Park, PAR = Parramatta, CAM = Campbelltown, PEN = Penrith.

	2000–2009						2010–2020					
	$\geq 35^\circ\text{C}$ (n)	$\geq 40^\circ\text{C}$ (n)	$\geq 45^\circ\text{C}$ (n)	#HW (n)	mean HW T_{max} ($^\circ\text{C}$)	abs T_{max} ($^\circ\text{C}$)	$\geq 35^\circ\text{C}$ (n)	$\geq 40^\circ\text{C}$ (n)	$\geq 45^\circ\text{C}$ (n)	#HW (n)	mean HW T_{max} ($^\circ\text{C}$)	abs T_{max} ($^\circ\text{C}$)
CBD	37	4	0	0 (0)	–	44.2	61	9	1	0 (0)	–	45.8
Oly	113	16	0	3 (4)	38.4 (± 2.5)	44.7	129	27	1	2 (3)	38.8 (± 3.1)	47.1
PaR	139	23	0	9 (4)	40.3 (± 2.3)	44.8	161	31	3	8 (6)	41.1 (2.7)	47.0
Cam	163	26	1	12 (5)	40.6 (± 2.1)	45.0	208	41	5	18 (7)	41.3 (± 2.6)	46.4
Pen	213	45	3	21 (6)	40.8 (± 2.3)	46.0	293	75	7	25 (9)	42.2 (± 2.7)	48.9

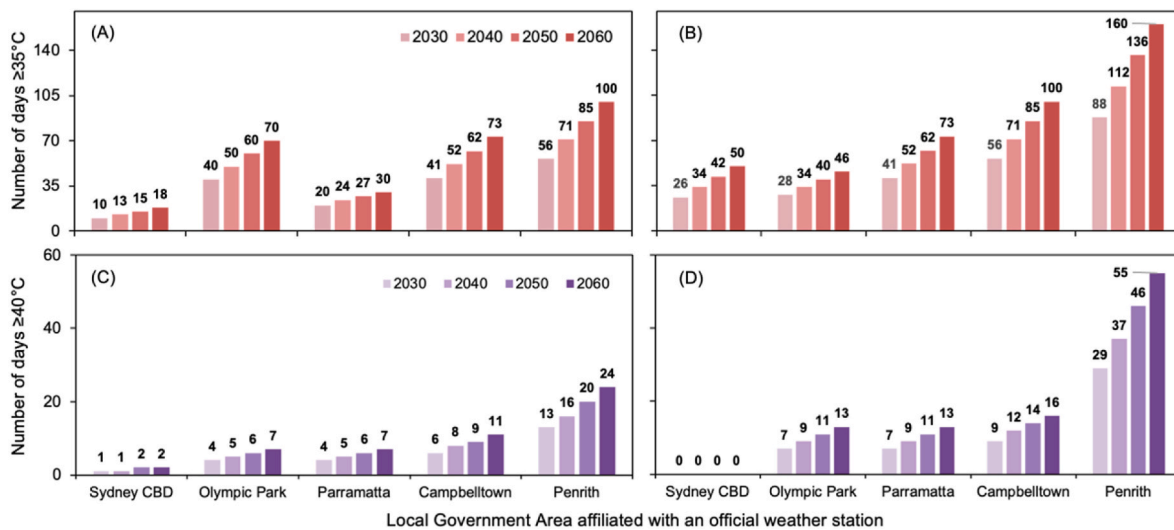


Fig. 4. Potential summer heat forecast across Greater Sydney. Number of hot ($T_{max} \geq 35^\circ\text{C}$, A, B) and extreme heat ($T_{max} \geq 40^\circ\text{C}$, C, D) days per year predicted for the next four decades based on measurements from five official weather stations spanning (A, C) 2000–2020 and (B, D) 2010–2020. Location of weather stations is ordered from east (left, coastal) to west (right, inland). Data from the weather station at Observatory Hill is used to represent Sydney CBD. The number of days is shown above each bar.

Table 3

Differences in maximum air temperatures (T_{max}) between Bureau of Meteorology (BoM) weather stations and air temperature loggers (ATLs). Data was recorded during January and February 2019 (Cumberland, Parramatta, Campbelltown) and 2020 (Penrith). HW = heatwave. Note: Data for hot and extreme heat days were aggregated based on measurement days and will vary from those that are aggregated using individual loggers.

Parameter	Cumberland		Parramatta		Campbelltown		Penrith	
	BoM	ATLs	BoM	ATLs	BoM	ATLs	BoM	ATLs
Absolute T_{max} ($^\circ\text{C}$)	40.2	45.2	39.2	43.0	40.9	44.8	48.9	52.0
Days $\geq 35^\circ\text{C}$ (n)	7	32	12	26	16	32	12	23
Days $\geq 40^\circ\text{C}$ (n)	1	15	0	7	3	15	6	8
Days $\geq 45^\circ\text{C}$ (n)	0	1	0	0	0	0	2	2
Min/max # of microsities (n) where $T_{max} >$ BoM station	–	25/75	–	8/37	–	14/64	–	7/58
Number of HW (n)	0	4	1	3	2	3	1	3
Duration of the longest HW (consecutive days)	0	5	3	4	4	10	4	5

$\geq 35^\circ\text{C}$ (presented as ‘ Δ Number of days’, Fig. 5) revealed novel patterns of the risk of underreporting summer heat across LGAs of Central and Western Sydney. In the LGAs of Cumberland (Fig. 5A) and Parramatta (Fig. 5B), underreporting of heat was widespread across western suburbs like Greystanes, Pemulwuy, Toongabbie or Wentworthville whereas eastern suburbs like Auburn, Eastwood and Olympic Park, were less prone to this risk. In the LGA of Parramatta, several measurement locations even had negative Δ values, indicating that ATLs had recorded fewer hot days than the official weather station. The number of hot days recorded by ATLs was also lower at the northern and southern ends of the LGA of Campbelltown (Fig. 5C) and the densely populated central section of the LGA of Penrith (Fig. 5D). The lowest number of hot days was recorded near Jinga Pools in the Dharawal National Park, southeast of Campbelltown ($\Delta = -10$). In contrast, the individual location with the largest number of unreported hot days ($\Delta = 21$) was in Smithfield at the southwestern end of the Cumberland LGA where it was surrounded by three large industrial estates.

On days where T_{max} recorded by BoM stations was $\geq 35^\circ\text{C}$ ($n = 47$), half of the microsities (49%) in each LGA recorded higher T_{max} . On these days, mean ΔT_{max} was $+4.0^\circ\text{C}$ (± 1.2 (± 1 Standard Deviation)) and the relationship of T_{max} between the BoM and ALT measurements was linear and highly significant ($p < 0.001$) (Fig. 6). The largest single difference of 6.9°C was measured on January 18, 2019 in Cumberland, where the closest BoM weather station at Olympic Park recorded T_{max} of 37.6°C and the ATL recorded 44.5°C .

4. Discussion

4.1. Impacts of heat in Western Sydney

Summer heat across Greater Sydney and especially Western Sydney has increased markedly in recent history and is likely to increase further in the coming decades. We showed that based on the trends of the past two decades, the number of hot (maximum air temperature $\geq 35^\circ\text{C}$) and extreme heat (maximum air temperature $\geq 40^\circ\text{C}$) days could more than double in the next three to four decades. Local populations of Western Sydney could experience entire summers (December to February) where maximum air temperature would be at or above 35°C every day, leading to growing heat stress (Vargas Zepetello et al., 2022). We recognise that the approach we have taken contains large uncertainty as several regressions to extrapolate the number of hot and extreme heat days from the past two decades into the future were not statistically significant. However, several regressions yielded highly significant relationships, all with positive slopes and intercepts that point towards increasing heat. It could be argued that our results may even underestimate the number hot and extreme heat days, when the exposure to heatwaves in the Sydney Region was predicted to increase 52-fold by 2100 using the RCP8.5-SSP5 pathway (Nishant et al., 2022). These predictions should be of great concern to health services, land managers, policy makers, and the wider public, as the positive relationship between heat and cost to the public health system is well established (Tong et al., 2021). The construction sector and private households will also be impacted.

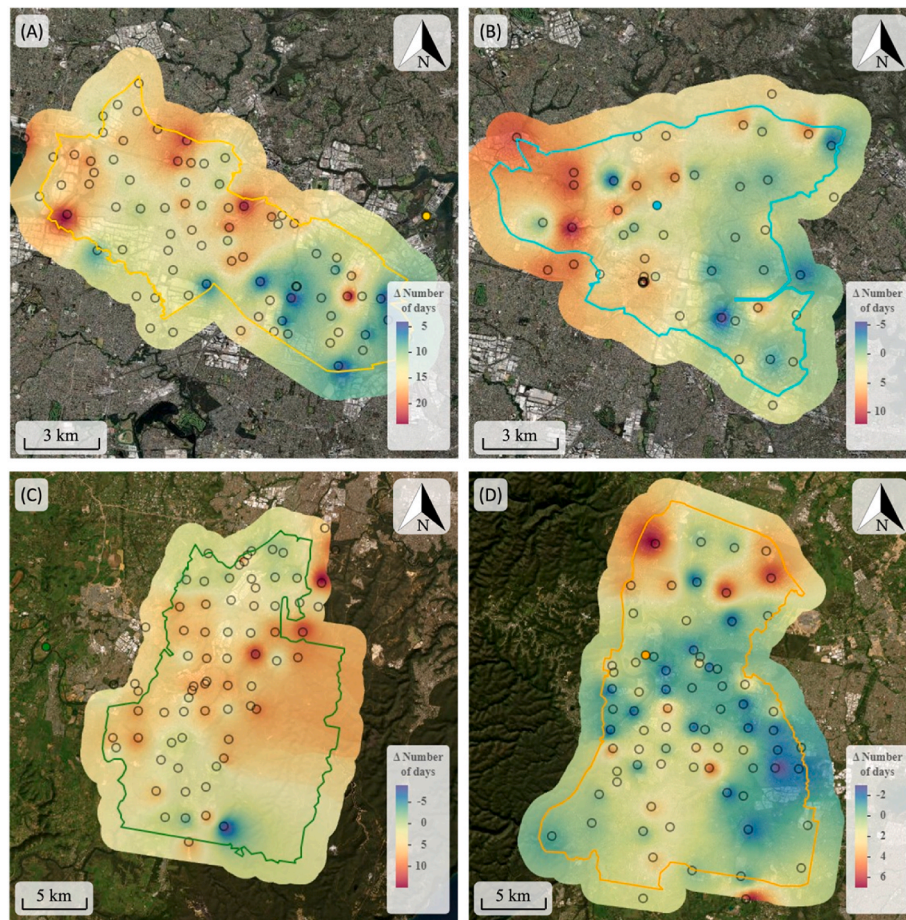


Fig. 5. ‘Heat risk’ maps. The risk of underreporting heat, represented by the differential (Δ) in the number of days where ATLS recorded $T_{\max} \geq 35$ °C compared to those from BoM stations. Positive values indicate that ATLS recorded more hot days, negative values indicate ATLS recorded fewer hot days than official weather stations. (A) Cumberland, (B) Parramatta, (C) Campbelltown, (D) Penrith. Boundaries of LGAs are shown as solid lines and their colour matches those in Fig. 1. Locations of ATLS are shown as circles and the nearest official weather stations are shown as coloured dots. See Material and Methods section for details of the spatial interpolation procedures used.

Economical modelling has indicated that extreme heat and associated expenses from deteriorating public health, rising cooling electricity needs, and losses in productivity across Western Sydney are currently costing businesses and the public AU\$1.44 billion, rising to AU\$5.94 billion by 2050 (Kernaghan, 2024).

The population of Western Sydney has been growing rapidly over the past two decades and this trend is predicted to continue. In 2023, around 2,734,000 residents lived in the region, and the population growth is estimated to be 1.64% annually for the next 15 years or more (NSW Government, 2022). Census data from the Australian Bureau of Statistics indicated that the population across Western Sydney is not only growing rapidly, but that it is also aging. It is thus reasonable to expect that more extreme heat will also lead to higher mortality in the elderly population (Coates et al., 2014) in Western Sydney. We note that our approach did not include effects on summer air temperatures that would likely originate from population growth and associated land use change. These relationships should be investigated in scenario models that assess the impact of urban development on regional climate (e.g., Zhou and Chen, 2018; Liu et al., 2024). Such studies are emerging, linking microclimatic variation of near-surface air temperatures to satellite-based data products that can be used to quantify thermal effects of land use change and progressing urbanisation (e.g., Chen et al., 2024; Burger et al., 2024), representing highly relevant information for a region like Central and Western Sydney where large-scale urban development will continue for decades.

A development that may impact local populations more broadly is

the declaration of ‘priority growth areas and precincts’ by the State Government (see <https://www.planning.nsw.gov.au/plans-for-your-area/priority-growth-areas-and-precincts>). Many of the areas where urban development is concentrated are in parts of Western Sydney that historically have the warmest summers. According to our analyses, areas of intense urban development will be exposed to increasingly adverse summer conditions in the coming decades. Kong et al. (2023) demonstrated that a 2020 heatwave in Sydney amplified surface urban heat island intensity at night by approximately 4 °C, and the impact was greater in urban areas than in rural areas. This important factor should be taken into account by urban planners when designing new developments (Peng et al., 2022; Ibsen et al., 2022), and heat mitigation techniques should be incorporated wherever possible. For example, inclusion of urban green and blue spaces (e.g., Imran et al., 2019; Georgescu et al., 2024) together with appropriate building design that uses wide eaves, light-coloured roofs (Bartesaghi-Koc et al., 2021) and optimal thermal insulation will assist in protecting people from extreme heat events in the future. A 1 °C increase in daytime temperature during an extreme heat event can increase mortality by 7.9% (Anderson and Bell, 2011), thus, even small reductions in intra-urban air temperature can have a positive effect in protecting people from heat-induced health problems.

When urban overheating coincides with extreme heat events, thermal stress is amplified even further (Khan et al., 2021). Our work extended previous analyses of the east-west air temperature gradient in Greater Sydney (e.g., Melville-Rea and Verschuer, 2022), showing that

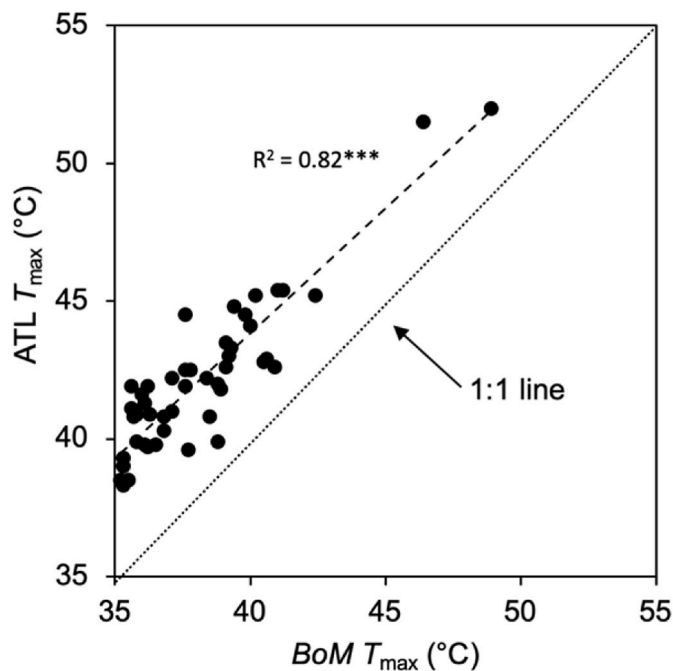


Fig. 6. Daily maximum air temperature (T_{\max}) recorded by the Bureau of Meteorology (BoM) weather stations and air temperature loggers (ATL) in the four local government areas. Only days in January and February 2019 and 2020, where the BoM station recorded $T_{\max} \geq 35$ °C are shown ($n = 47$). The dotted 1:1 line shows where T_{\max} of the BoM and ATLs would be equal. Best fit function (dashed line) and the coefficient of determination are shown; *** indicate a highly significant relationship ($p < 0.001$).

the thermal gradient also applies in a southerly direction. Heatwaves in the far west of Greater Sydney (i.e., LGA of Penrith) have been more frequent, longer, and hotter during the last 15 years than in other LGAs studied. Campbelltown in the southwest had also recorded more heatwave events of longer duration and greater intensity than Parramatta and Cumberland in the central region, suggesting that the people living in the western and southern parts of Greater Sydney are likely to be at greater risk from heatwaves in the future. By contrast, there were no heatwaves recorded in the CBD of Sydney between 2007 and 2021. Our projection for extreme heat days for the Sydney's CBD also showed no increase of extreme heat days, though this prediction is admittedly based on considerably large year-to-year variability in the number of hot and extreme heat days.

Heatwave development and dissipation across Greater Sydney are strongly influenced by two synoptic weather patterns - the build-up of hot air from the north-west, and movement of cool air from a southern cold front (Sadeghi et al., 2018; He et al., 2020; Pfautsch et al., 2020). While the coastal suburbs experience cooling sea breezes that can reduce the intensity and frequency of heatwaves, areas in the outer west and south lack this natural cooling effect, resulting in more intense and longer lasting heat events (Steffen and Hughes, 2012). Based on our microclimate measurements, differences in maximum air temperature during heatwaves in the CBD of Sydney compared to Western Sydney were as high as 17 °C. These deviations demonstrate that BoM stations underreport extreme heat experienced by local populations.

4.2. Recommendations

The broader recognition of potentially serious impacts of extreme heat events on human health (Wang et al., 2022) has led to the development and implementation of heat-health watch and early warning systems to mitigate exposure in many countries (Issa et al., 2021). These systems are vital for protecting human populations from the impacts of

heatwaves and extreme heat events in the future (Kotharkar et al., 2022). Such warning systems usually draw data from official weather station networks within a city (Nitschke et al., 2016; Casanueva et al., 2019). As detected in our study, if microclimatic variation across urban landscapes is more widespread and greater in amplitude than previously documented by official weather stations, two important issues arise.

First, local populations and businesses are prone to experiencing a growing, yet undetected risk of exposure to the impacts of more hot and extreme heat days. This, in turn, leads to an incapacity to issue warnings and control the associated risks experienced by local populations and businesses. At the local level, the combination of more heat and limited preparedness represents a growing risk for public health (Ebi et al., 2021) and work safety (Deshayes et al., 2024). It is thus recommended that the urgent problem of underreporting of summer heat is addressed immediately not only in Western Sydney, but in metropolitan regions more broadly where urban densification and expansion intensifies daytime heat and CLUHI effects (Chapman et al., 2017; Santamouris et al., 2017). Here we presented novel 'heat risk' maps that identify regions and suburbs where underreporting of summer heat is frequent. Such maps, based on empirical measurements from microsites and official weather stations, can be used to communicate the risk to government agencies as well as the public to improve heat preparedness and focus resources to areas where interventions to mitigate summer heat will be needed.

Second, in addition to the existing network of weather stations, it is recommended that government authorities establish a network of weather sensors in the most heat affected locations to capture weather measurements at much higher granularity. Potential static and dynamic solutions for such networks are discussed in the literature (e.g., Muller et al., 2013; Meier et al., 2017; Song et al., 2022; Chen and Yang, 2022).

Human health and wellbeing do not depend only on air temperature. Outcomes are influenced by other meteorological variables including solar radiation, relative humidity, and radiant heat, which are often overlooked (e.g., Casanueva et al., 2019; Baldwin et al., 2023). A warming climate is increasing the amount of water vapour in the atmosphere by about 6–7% per degree or warming (Sherwood and Ram-say, 2023). Predictions of spatial changes of relative humidity in Australia vary, depending largely on underlying greenhouse gas emission scenarios, with some areas expected to become more, others less humid (ARC Centre for Excellence in Climate Extremes, 2023). Studies investigating the spatial variation of additional meteorological variables would be useful, yet instrumentation for such studies is currently missing at meaningful intra-urban scales. Another parameter that impacts public health in cities is air pollution. A citizen-focussed sensor network has been established across schools in Greater Sydney to monitor heat and air pollution (Ulpiani et al., 2022), yet its granularity is limited. However, it is initiatives like these that can act as foundational projects for larger intra-urban monitoring and reporting networks.

5. Conclusion

Based on historical weather data and empirical measurements of near-surface air temperature at several hundred locations across Central and Western Sydney, we were able to show that the region is rapidly warming. Forward trajectories of extreme heat events show that the level of broadscale warming could lead to highly challenging conditions for millions of people when extreme heat becomes commonplace in summers during the next 30–40 years. We identified that intra-urban heat is commonly underreported by the official weather stations across Greater Sydney. We conclude that predictive heat modelling to issue public warning messages will be insufficient to protect urban populations from heat-related risks. Sensor networks with high granularity can provide the necessary micrometeorological information and novel visualisations of data recorded by these networks will assist in communicating risks arising from unexpected heat exposure. At the same time, it is important to develop effective adaptation strategies for

cities and their communities. This applies to Greater Sydney and many other metropolitan regions in Australia and elsewhere.

CRedit authorship contribution statement

Sebastian Pfautsch: Writing – original draft, Visualization, Methodology, Funding acquisition, Formal analysis, Conceptualization. **Agnieszka Wujeska-Klaue:** Writing – review & editing, Formal analysis, Data curation. **Judi R. Walters:** Writing – review & editing.

Funding

This research was funded by the local governments of Parramatta City, Cumberland City, Campbelltown City and Penrith City, Australia.

Declaration of competing interest

The authors declare that they have no known competing financial interests or personal relationships that could have appeared to influence the work reported in this paper.

Acknowledgments

The authors thank Susanna Rouillard for technical support.

Appendix A. Supplementary data

Supplementary data to this article can be found online at <https://doi.org/10.1016/j.wace.2024.100741>.

Data availability

Data will be made available on request.

References

- Adnan, M.S.G., Dewan, A., Botje, D., Shahid, S., Hassan, Q.K., 2022. Vulnerability of Australia to heatwaves: a systematic review on influencing factors, impacts, and mitigation options. *Environ. Res.* 213, 11373. <https://doi.org/10.1016/j.envres.2022.113703>.
- Anderson, G.B., Bell, M.L., 2011. Heat waves in the United States: mortality risk during heat waves and effect modification by heat wave characteristics in 43 US communities. *Environ. Health Perspect.* 119, 210–218. <https://doi.org/10.1289/ehp.1002313>.
- ARC for Excellence for Climate Extremes, 2023. Projecting future heat stress in Australia using climate models. Available at: <https://climateextremes.org.au/projecting-future-heat-stress-in-australia-using-climate-models-2/>.
- Asseng, S., Spankuch, D., Hernandez-Ochoa, I.M., Laporta, J., 2021. The upper temperature thresholds of life. *Lancet Planet. Health* 5, e378–e385. [https://doi.org/10.1016/S2542-5196\(21\)00079-6](https://doi.org/10.1016/S2542-5196(21)00079-6).
- Back, J., Kumar, P., Bach, P.M., Rauch, W., Kleindorfer, W., 2023. Integrating CFD-GIS modelling to refine urban heat and thermal comfort assessment. *Sci. Total Environ.* 858, 159729. <https://doi.org/10.1016/j.scitotenv.2022.159729>.
- Bahi, H., Mastouri, H., Radoine, H., 2020. Review of methods for retrieving urban heat islands. *Mater. Today: Proc.* 27, 3004–3009. <https://doi.org/10.1016/j.matpr.2020.03.272>.
- Baldwin, J.W., Benmarhnia, T., Ebi, K.L., Jay, O., Lutsko, N.J., Vanos, J.K., 2023. Humidity's role in heat-related health outcomes: a heated debate. *Eviron. Health Persp.* 131, 055001. <https://doi.org/10.1289/EHP11807>.
- Ballester, J., Quijal-Zamorano, M., Méndez Turrubiates, R.F., Pegenaute, F., Herrmann, F.R., Robine, J.M., Basagaña, X., Tonne, c., Antó, J.M., Achebak, H., 2023. Heat-related mortality in Europe during the summer of 2022. *Nat. Med.* (N. Y., NY, U. S.) 29, 1857–1866. <https://doi.org/10.1038/s41591-023-02419-z>.
- Bartasaghi-Koc, C., Haddad, S., Pignatta, G., Paolini, R., Prasad, D., Santamouris, M., 2021. Can urban heat be mitigated in a single urban street? Monitoring, strategies, and performance results from a real scale redevelopment project. *Sol. Energy* 216, 564–588. <https://doi.org/10.1016/j.solener.2020.12.043>.
- Bassil, K.L., Colet, D.C., 2010. Effectiveness of public health interventions in reducing morbidity and mortality during heat episodes: a structured review. *Int. J. Environ. Res. Publ. Health* 7, 991–1001. <https://doi.org/10.3390/ijerph7030991>.
- Bureau of Meteorology, 2021. Annual climate summary for greater Sydney. Available at: <http://www.bom.gov.au/climate/current/annual/nsw/sydney.shtml>. (Accessed 9 October 2024).
- Bureau of Meteorology, 2022a. What is a heatwave. Available at: <http://www.bom.gov.au/australia/heatwave/knowledge-centre/understanding.shtml>. (Accessed 20 April 2024).
- Bureau of Meteorology, 2022b. Heatwave services. <http://www.bom.gov.au/australia/heatwave/knowledge-centre/heatwave-service.shtml>. (Accessed 20 April 2024).
- Burger, M., Gubler, M., Brönnimann, S., 2024. High-resolution dataset of nocturnal air temperatures in Bern, Switzerland (2007–2022). *Geosci. Data J.* 00 1–15. <https://doi.org/10.48620/316>.
- Casanueva, A., Burgstall, A., Kotlarski, S., Messeri, A., Morabito, M., Flouris, A.D., Nybo, L., Spring, C., Schwierz, C., 2019. Overview of existing heat-health warning systems in Europe. *Int. J. Environ. Res. Publ. Health* 16, 2657. <https://doi.org/10.3390/ijerph16152657>.
- Cecilia, A., Cassasanta, G., Petenko, I., Conidi, A., Argenti, S., 2023. Measuring the urban heat island of Rome through a dense weather station network and remote sensing imperviousness data. *Urban Clim.* 47, 101355. <https://doi.org/10.1016/j.uclim.2022.101355>.
- Chapman, S., Watson, J.E.M., Salazar, A., Thatcher, M., McAlpine, C.A., 2017. The impact of urbanization and climate change on urban temperatures: a systematic review. *Landsc. Ecol.* 32, 1921–1935. <https://doi.org/10.1007/s10980-017-0561-4>.
- Chaston, T.B., Broome, R.A., Cooper, N., Duck, G., Geromboux, C., Guo, Y., Ji, F., Perkins-Kirkpatrick, S., Zhang, Y., Dissanayake, G.S., Morgan, G.G., Hanigan, I.C., 2022. Mortality burden of heatwaves in Sydney, Australia is exacerbated by the urban heat island and climate change: can tree cover help mitigate the health impacts? *Atmosphere* 13, 714. <https://doi.org/10.3390/atmos13050714>.
- Chen, Y.-C., Hou, K.-S., Lioa, Y.-J., Honjo, T., Cheng, F.-Y., Lin, T.-P., 2024. The application of a high-density street-level air temperature observation network (HiSAN): spatial and temporal variations of thermal and wind condition in different climatic condition types. *Sustain. Cities Environ.* 109, 105547. <https://doi.org/10.1016/j.scs.2024.105547>.
- Chen, X., Yang, J., 2022. Urban climate monitoring network design: existing issues and a cluster-based solution. *Build. Environ.* 214, 108959. <https://doi.org/10.1016/j.buildenv.2022.108959>.
- Coates, L., Haynes, K., O'Brien, J., McAnaney, J., de Oliveira, F.D., 2014. Exploring 167 years of vulnerability: an examination of extreme heat events in Australia 1844–2010. *Environ. Sci. Pol.* 42, 33–44. <https://doi.org/10.1016/j.envsci.2014.05.003>.
- Deshayes, T.A., Hsouna, H., Braham, M.A.A., Arvisais, D., Pageaux, B., Ouellet, C., Jay, O., Maso, F.D., Begon, M., Saidi, A., Gendron, P., Ganon, D., 2024. Work-rest regimes for work in hot environments: a scoping review. *Am. J. Ind. Med.* 67, 304–320. <https://doi.org/10.1002/ajim.23569>.
- Donateo, A., Palusci, O., Pappacogli, G., Esposito, A., Martilli, A., Santiago, J.L., Buccolieri, R., 2023. Analysis of urban heat island and human thermal comfort in a Mediterranean city: a case study of Lecce (Italy). *Sustain. Cities Soc.* 98, 104849. <https://doi.org/10.1016/j.scs.2023.104849>.
- Ebi, K., Capon, A., Berry, P., Broderick, C., de Dear, R., Havenith, G., Honda, Y., Kovats, R.S., Ma, W., Malik, A., Morris, N.B., Nybo, L., Seneviratne, S.I., Vanos, J., Jay, O., 2021. Hot weather and heat extremes: health risks. *Lancet* 398, 698–708. [https://doi.org/10.1016/S0140-6736\(21\)01208-3](https://doi.org/10.1016/S0140-6736(21)01208-3).
- Gee, K., Gissing, A., 2021. Heat smart: building resilience to heatwaves in western Sydney. *Aust. J. Emerg. Manag.* 36, 5–7. <https://doi.org/10.3316/ajis.20211218058582>.
- Georgescu, M., Broadbent, A.M., Krayenhoff, E.S., 2024. Quantifying the decrease in heat exposure through adaptation and mitigation in twenty-first-century US cities. *Nature Cities* 1, 42–50. <https://doi.org/10.1038/s44284-023-00001-9>.
- Gubler, M., Christen, A., Remund, J., Bronnimann, S., 2021. Evaluation and application of a low-cost measurement network to study intra-urban temperature differences during summer 2018 in Bern, Switzerland. *Urban Clim.* 37, 100817. <https://doi.org/10.1016/j.uclim.2021.100817>.
- He, B.J., Ding, L., Prasad, D., 2020. Outdoor thermal environment of an open space under sea breeze: a mobile experience in a coastal city of Sydney, Australia. *Urban Clim.* 31, 100567. <https://doi.org/10.1016/j.uclim.2019.100567>.
- Herron, N.F., McVicar, T.R., Rohead-O'Brien, H., Rojas, R., Rachakonda, P.K., Zhang, Y. Q., Dawes, W.R., Macfarlane, C., Pritchard, J., Doody, T., Marvanek, S.P., Li, L.T., 2018. Context statement for the Sydney Basin bioregion. Product 1.1 from the Sydney Basin Bioregional Assessment. Department of the Environment and Energy, Bureau of Meteorology. CSIRO and Geoscience Australia, Australia, p. 182p.
- Honjo, T., Yamato, H., Mikami, T., Grimmond, C.S.B., 2015. Network optimization for enhanced resilience of urban heat island measurements. *Sustain. Cities Soc.* 19, 319–330. <https://doi.org/10.1016/j.scs.2015.02.004>.
- Hughes, L., Steffen, E., Mullins, G., Dean, A., Weisbrot, E., Rice, M., 2020. Summer of crisis. Climate Council of Australia Limited. <https://www.climatecouncil.org.au/resources/summer-of-crisis/> (accessed 20 April 2024).
- Ibsen, P.C., Janerette, G.D., Dell, T., Bagstad, K.J., Diffendorfer, J.E., 2022. Urban landcover differentially drives day and nighttime air temperature across a semi-arid city. *Sci. Total Environ.* 829, 154589. <https://doi.org/10.1016/j.scitotenv.2022.154589>.
- Imran, H.M., Kala, J., Ng, A.W.M., Muthukumaran, S., 2019. Effectiveness of vegetated patches as green infrastructure in mitigating urban heat island effects during a heatwave even in the city of Melbourne. *Weather Clim. Extrem.* 25, 100217. <https://doi.org/10.1016/j.wace.2019.100217>.
- IPCC, 2023. Summary for policymakers. In: Lee, H., Romero, J. (Eds.), *Climate Change 2023: Synthesis Report. Contribution of Working Groups I, II and III to the Sixth Assessment Report of the Intergovernmental Panel on Climate Change* [Core Writing Team, IPCC, p. 34p. <https://doi.org/10.59327/IPCC/AR6-9789291691647.001>. Geneva, Switzerland.

- Issa, M.A., Chebana, F., Massekot, P., Campagna, C., Lavigne, E., Gosselin, P., Ouarda, T. B.M.J., 2021. A heat-health watch and warning system with extended season and evolving thresholds. *BMC Publ. Health* 21, 1479. <https://doi.org/10.1186/s12889-021-10982-8>.
- Jyoteeshkumar Reddy, P., Perkins-Kirkpatrick, S.E., Sharples, J.J., 2021. Intensifying Australian heatwave trends and their sensitivity to observational data. *Earth's Future* 9, e2020EF001924. <https://doi.org/10.1029/2020EF001924>.
- Kernaghan, S., 2024. Burning Money – the Rising Costs of Heatwaves to Western Sydney. Committee for Sydney, p. 40p. https://a21234.hostroomcdn.com/wp-content/uploads/2024/03/Committee_for_Sydney_Burning_Money_March_2024.pdf. (Accessed 10 April 2024).
- Khan, H.S., Santamouris, M., Paolini, R., Caccetta, P., Kassomenos, P., 2021. Analyzing the local and climatic conditions affecting the urban overheating magnitude during heatwaves (HWs) in a coastal city: a case study of the greater Sydney region. *Sci. Total Environ.* 755, 142515. <https://doi.org/10.1016/j.scitotenv.2020.142515>.
- Khatana, S.A.M., Werner, R.M., Groeneveld, P.W., 2022. Association of extreme heat with all-cause mortality in the contiguous US, 2008–2017. *JAMA Netw. Open* 5, e2212957. <https://doi.org/10.1001/jamanetworkopen.2022.12957>.
- Kong, J., Zhao, Y., Strebel, D., Gao, K., Carmeliet, J., Lei, C., 2023. Understanding the impact of heatwave on urban heat in greater Sydney: temporal surface energy budget change with land types. *Sci. Total Environ.* 903, 166374. <https://doi.org/10.1016/j.scitotenv.2023.166374>.
- Kotharkar, R., Gosh, A., Arch, M., 2022. Progress in extreme heat management and warning systems: a systematic review of heat-health action plans (1995–2020). *Sustain. Cities Soc.* 76, 103487. <https://doi.org/10.1016/j.scs.2021.103487>.
- Li, H., Zhao, Y., Bardhan, R., Chan, P.W., Derome, D., Luo, Z., Urge-Vorsatz, D., Carmeliet, J., 2023. Relating three-decade surge in space cooling demand to urban warming. *Environ. Res. Lett.* 18, 124033. <https://doi.org/10.1088/1748-9326/ad0a56>.
- Li, Y., Yang, T., Zhao, G., Ma, C., Yan, Y., Xu, Y., Wang, L., Wang, L., 2024. A systematic review of studies involving canopy layer urban heat island: monitoring and associated factors. *Ecol. Indic.* 158, 111424. <https://doi.org/10.1016/j.ecolind.2023.111424>.
- Liu, Y., An, Z., Ming, Y., 2024. Simulating influences of land use/land cover composition and configuration on urban heat island using machine learning. *Sustain. Cities Soc.* 108, 105482. <https://doi.org/10.1016/j.scs.2024.105482>.
- Livada, I., Synnefa, A., Haddad, S., Paolini, R., Garshabi, S., Ulpiani, G., Fiorito, F., Vassilakopoulou, K., Osmond, P., Santamouris, M., 2019. Time series analysis of ambient air-temperature during the period 1970–2016 over Sydney, Australia. *Sci. Total Environ.* 648, 1627–1638. <https://doi.org/10.1016/j.scitotenv.2018.08.144>.
- Lu, P., Zhao, Q., Xia, G., Xu, R., Hanna, L., Jiang, J., Li, S., Guo, Y., 2021. Temporal trends of association between ambient temperature and cardiovascular mortality: a 17-year case-crossover study. *Environ. Res. Lett.* 16, 045004. <https://doi.org/10.1088/1748-9326/abab33>.
- Madrigano, J., Ito, K., Johnson, S., Kinney, P., Matte, T., 2015. A case-only study of vulnerability to heat wave-related mortality in New York City (2000–2011). *Environ. Health Perspect.* 123, 672–678. <https://doi.org/10.1289/ehp.1408178>.
- Marinaccio, A., Scortichini, M., Gariazzo, C., Leva, A., et al., 2019. Nationwide epidemiological study for estimating the effect of extreme outdoor temperature on occupational injuries in Italy. *Environ. Int.* 133, 105176. <https://doi.org/10.1016/j.envint.2019.105176>.
- Marks, D., Connell, J., 2023. Unequal and unjust: the political ecology of Bangkok's increasing urban heat island. *Urb. Studies* 61, 2887–2907. <https://doi.org/10.1177/00420980221140999>.
- Meier, F., Fenner, D., Grassmann, T., Otto, M., Scherer, D., 2017. Crowdsourcing air temperature from citizen weather stations for urban climate research. *Urban Clim.* 19, 170–191. <https://doi.org/10.1016/j.uclim.2017.01.006>.
- Melville-Rea, H., Verschuer, R., 2022. HeatWatch: Extreme Heat in Western Sydney, vol. 28p. The Australia Institute. <https://australianinstitute.org.au/wp-content/uploads/2022/01/HeatWatch-2022-WEB.pdf>. (Accessed 20 April 2024).
- Muller, C.L., Chapman, L., Grimmond, C.S.B., Young, D.T., Cai, X., 2013. Sensors and the city: a review of urban meteorological networks. *Int. J. Climatol.* 33, 1585–1600. <https://doi.org/10.1002/joc.3678>.
- Nishant, N., Ji, F., Guo, Y., Herold, N., Green, D., Di Virgilio, G., Bayer, K., Riley, M.L., Perkins-Kirkpatrick, S., 2022. Future population exposure to Australian heatwaves. *Environ. Res. Lett.* 17, 064020. <https://doi.org/10.1088/1748-9326/ac6dfa>.
- Nitschke, M., Tucker, G., Hansen, A., Williams, S., Zhang, Y., Bi, P., 2016. Evaluation of a heat warning system in Adelaide, South Australia, using case-series analysis. *BMJ Open* 6, 012125. <https://doi.org/10.1136/bmjopen-2016-012125>.
- NSW Government, 2022. NSW Government planning portal. Available at: <https://pp.planningportal.nsw.gov.au/populations>. (Accessed 20 April 2024).
- Peng, W., Wang, R., Duan, J., Gao, W., Fan, Z., 2022. Surface and canopy urban heat islands: does urban morphology result in spatiotemporal differences? *Urban Clim.* 42, 101136. <https://doi.org/10.1016/j.uclim.2022.101136>.
- Pfautsch, S., Rouillard, S., 2019a. Benchmarking Heat across Cumberland Council, New South Wales. Western Sydney University and Cumberland City Council. <https://doi.org/10.26183/5d76e1fa3b31a>.
- Pfautsch, S., Rouillard, S., 2019b. Benchmarking Heat in Parramatta, Sydney's Central River City. Western Sydney University and Parramatta City Council. <https://doi.org/10.26183/5d4b69d465d6d6>.
- Pfautsch, S., Wujeska-Klaue, A., Rouillard, S., 2020. Benchmarking Summer Heat across Penrith, New South Wales. Western Sydney University and Penrith City Council. <https://doi.org/10.26183/44va-ck37>.
- Pfautsch, S., Wujeska-Klaue, A., Walters, J., 2023. Measuring local-scale canopy-layer air temperatures in the built environment: a flexible method for urban heat studies. *Comput. Environ. Urban Syst.* 99, 101913. <https://doi.org/10.1016/j.compenurbysys.2022.101913>.
- Potgieter, J., Nazarian, N., Lipson, M.J., Hart, M.A., Ulpiani, G., Morrison, W., Benjamin, K., 2021. Combining high-resolution land use data with crowdsourced air temperature to investigate intra-urban microclimate. *Front. Environ. Sci.* 9, 720323. <https://doi.org/10.3389/fenvs.2021.720323>.
- Richard, Y., Pohl, B., Rega, M., Pergaud, J., Thevenin, T., Emery, J., Dudek, J., Vairet, T., Zito, S., Chateau-Smith, C., 2021. Is urban heat island intensity higher during hot spells and heat waves (Dijon, France, 2014–2019)? *Urb. Clim. Past* 35, 100747. <https://doi.org/10.1016/j.uclim.2020.100747>.
- Sadeghi, M., de Dear, R., Wood, G., Samali, B., 2018. Development of a bioclimatic wind rose tool for assessment of comfort wind resources in Sydney, Australia for 2013 and 2030. *Int. J. Biometeorol.* 62, 1963–1972. <https://doi.org/10.1007/s00484-018-1597-0>.
- Santamouris, M., Haddad, S., Fiorito, F., Osmond, P., Ding, L., Prasad, D., Zhai, X., Wang, R., 2017. Urban heat island and overheating characteristics in Sydney, Australia. An analysis of multiyear measurements. *Sustainability* 9, 712. <https://doi.org/10.3390/su9050712>.
- Sherwood, S.C., Huber, M., 2010. An adaptability limit to climate change due to heat stress. *Proc. Natl. Acad. Sci. USA* 107, 9552–9555. <https://doi.org/10.1073/pnas.0913352107>.
- Sherwood, S.C., Ramsay, E.E., 2023. Closer to limits of human tolerance of global heat. *Proc. Natl. Acad. Sci. USA* 120 (43), e2316003120. <https://doi.org/10.1073/pnas.2316003120>.
- Singh, V.K., Mohan, M., Bhati, S., 2023. Industrial heat island mitigation in Angul-Talcher Region of India: evaluation using modified WRF-single urban canopy model. *Sci. Total Environ.* 858, 159949. <https://doi.org/10.1016/j.scitotenv.2022.159949>.
- Song, K., Liu, X., Gao, T., 2022. Potential application of using smartphone sensor for estimating air temperature: experimental study. *IEEE Internet Things J.* 9, 14300–14306. <https://doi.org/10.1109/JIOT.2021.3063488>.
- Steffen, W., Hughes, L., 2012. The critical decade: New South Wales climate impacts and opportunities. Available at: Commonwealth of Australia, Climate Commission Secretariat. Department of Climate Change and Energy Efficiency, p. 28. <https://researchers.mq.edu.au/files/72295355/72295318.pdf> (accessed 20 April 2024).
- Steffen, W., Hughes, L., Mullins, G., Bambrick, H., Dean, A., Rice, M., 2019. Dangerous summer: escalating bushfire, heat and drought risk. Climate Council of Australia. <https://www.climatecouncil.org.au/resources/dangerous-summer-escalating-bush-fire-heat-drought-risk/>. (Accessed 20 April 2024).
- Stewart, I.D., Oke, T.R., 2012. Local Climate Zones for urban temperature studies. *Bull. Am. Meteorol. Soc.* 93. <https://doi.org/10.1175/BAMS-D-11-00019.1>, 1879–190.
- Stone, J.R.B., Gronlund, C.J., Mallen, E., Hondula, D., O'Neill, M.S., Rajput, M., Grijalva, S., Lenza, K., Harlan, S., Larsen, L., Augenbroe, G., Krayenhoff, E.S., Broadbent, A., Georgescu, M., 2023. How blackouts during heat waves amplify mortality and morbidity risk. *Environ. Sci. Technol.* 57, 8245–8255.
- Tong, M.Z., Wondmagegn, B.Y., Ziang, J., Williams, S., Hansen, A., Dear, K., Pisaniello, D., Xiao, J., Jian, L., Scalley, B., Nitschke, M., Nairn, J., Bambrick, H., Karnon, J., Bi, P., 2021. Emergency department visits and associated healthcare costs attributable to increasing temperature in the context of climate change in Perth, Western Australia, 2012–2019. *Environ. Res. Lett.* 16, 065011. <https://doi.org/10.1088/1748-9326/ac04d5>.
- Trancoso, R., Syktus, J., Toombs, N., Ahrens, D., Wong, K.K.-H., Pizza, R.D., 2020. Heatwaves intensification in Australia: a consistent trajectory across past, present and future. *Sci. Total Environ.* 742, 140521. <https://doi.org/10.1016/j.scitotenv.2020.140521>.
- Ulpiani, G., Ranzi, G., Santamouris, M., 2021. Local synergies and antagonisms between meteorological factors and air pollution: a 15-year comprehensive study in the Sydney region. *Sci. Total Environ.* 788, 147783. <https://doi.org/10.1016/j.scitotenv.2021.147783>.
- Ulpiani, G., Hart, M.A., DiVirgilio, G., Maharaj, A.M., Lipson, M.J., Potgieter, J., 2022. A citizen centered urban network for weather and air quality in Australian schools. *Sci. Data* 9, 129. <https://doi.org/10.1038/s41597-022-01205-9>.
- Vargas Zepetello, L.R., Raftery, A.E., Battisti, D.S., 2022. Probabilistic projections of increased heat stress driven by climate change. *Communic. Earth Environ* 3, 183. <https://doi.org/10.1038/s4347-022-0052-4>.
- Vicedo-Cabrera, A.M., Scovronick, N., Sera, F., Roye, D., Schneider, R., Tobias, A., Astronom, C., Gui, Y., Honda, Y., Hondula, D.M., Abutzky, R., Tong, S., de Sousa Zanotti Stagliorio Coelho, M., Nascimento Saldiva, P.H., Lavigne, E., Matus Correa, P., Valdes Ortega, N., Kan, H., Osorio, S., et al., 2021. The burden of heat-related mortality attributable to recent human-induced climate change. *Nat. Clim. Change* 11, 492–500. <https://doi.org/10.1038/s41558-021-01058-x>.
- Wang, X.-S., He, L., Ma, X.H., Bie, Q., Luo, L., Xiong, Y.-C., Ye, J.-S., 2022. The emergence of prolonged deadly humid heatwaves. *Int. J. Climatol.* 1–12, 7750. <https://doi.org/10.1002/joc.7750>.
- Weather Spark, 2022. Climate and average weather year round in Sydney, Australia. Available at: <https://weatherspark.com/y/144544/Average-Weather-in-Sydney-Australia-Year-Round>. (Accessed 20 April 2024).
- WMO, 2018. World Meteorological Society. Guide to instruments and methods of observation. Vol. 1 - Measurement of Meteorological Variables, eighteenth ed. WMO, Geneva, Switzerland.
- Yenneti, K., Ding, L., Prasad, D., Ulpiani, G., Paolini, R., Haddad, S., Santamouris, M., 2020. Urban overheating and cooling potential in Australia: an evidence-based review. *Climate* 8, 126. <https://doi.org/10.3390/cli8110126>.
- Yin, S., Xiao, S., Ding, X., Fan, Y., 2024. Improvement of spatial-temporal urban heat island study based on local climate zone framework: a case study of Hangzhou, China. *Build. Environ.* 248, 111102. <https://doi.org/10.1016/j.buildenv.2023.111102>.

- Yun, G.Y., Ngarambe, J., Dahirwe, P.N., Ulpiani, G., Paolini, R., Haddad, S., Vasilakopoulou, K., Santamouris, M., 2020. Predicting the magnitude and the characteristics of the urban heat island in coastal cities in the proximity of desert landforms. The case of Sydney. *Sci. Total Environ.* 709, 136068. <https://doi.org/10.1016/j.scitotenv.2019.136068>.
- Zanobetti, A., O'Neill, M.S., Gronlund, C.J., Schwartz, J.D., 2013. Summer temperature variability and long-term survival among elderly people with chronic disease. *Proc. Natl. Acad. Sci. USA* 109, 6608–6613. <https://doi.org/10.1073/pnas.1113070109>.
- Zhou, X., Chen, H., 2018. Impact of urbanization-related land use cover changes and urban morphology changes on the urban heat island phenomenon. *Sci. Total Environ.* 635, 1467–1476. <https://doi.org/10.1016/j.scitotenv.2019.136068>.
- Zhu, H.-C., Ren, C., Wang, J., Feng, Z., Haghighat, F., Cao, S.-J., 2024. Fast prediction of spatial temperature distributions in urban areas with WRF and temporal fusion transformers. *Sust. Cities Environ.* 103, 105249. <https://doi.org/10.1016/j.scs.2024.105249>.
- Zumwald, M., Knüsel, B., Bresch, D.N., Knutti, R., 2021. Mapping urban temperature using crowd-sensing data and machine learning. *Urban Clim.* 35, 100739. <https://doi.org/10.1016/j.uclim.2020.100739>.